ELSEVIER

Catalysis Today 49 (1999) 339–352

CATALYSIS TODAY

Toroid NMR probes for the in situ examination of homogeneous cobalt hydroformylation catalysts at high pressures and temperatures

Kurt W. Kramarz, Robert J. Klingler, David E. Fremgen, Jerome W. Rathke*

Argonne National Laboratory, 9700 South Cass Avenue, Argonne, IL 60439, USA

Abstract

Toroid NMR probes can be routinely operated at 300 atm and up to 250°C. Such operating conditions make these probes well suited for the in situ examination of catalytic industrial processes. These probes have been employed to examine phosphine substituted (Shell-type) and unsubstituted cobalt carbonyl oxo catalysts under catalytic and non-catalytic conditions in a variety of solvents. The solvents include cyclohexane, benzene, dioxane, 2-methylpropanol, supercritical carbon dioxide ($scCO_2$), and $scCO_2$/toluene mixtures. The high-pressure/high-temperature probes allowed the observation of precatalytic equilibria under high carbon monoxide pressures in the presence and absence of hydrogen and/or free phosphine. © 1999 Elsevier Science B.V. All rights reserved.

1. Introduction

The use of nuclear magnetic resonance (NMR) spectroscopy for the examination of both organic and inorganic chemical species has led to some of the greatest advances in homogeneous catalysis. However, until recently, in situ high-pressure and high-temperature techniques had not been employed routinely to obtain data upon catalysts under extreme industrial process conditions. We report here in situ high-pressure studies of phosphine-modified cobalt carbonyl hydroformylation catalysts with a toroid NMR probe.

Three approaches have been successfully employed to obtain high-pressure fluid-phase NMR spectra: (1) sapphire NMR tubes, (2) capillary NMR tube cells, and (3) metallic vessel NMR probes. A review of high-pressure techniques, including NMR, has been recently published [1].

Sapphire NMR tubes allow the use of relatively thin-walled NMR tubes and was pioneered by Roe [2] with modifications by others [3,4]. The advantage of this technique is the ability to spin the high-pressure sample in a commercial NMR spectrometer probe. The disadvantage of the sapphire NMR tube is the unpredictability of pressure limitations due to the existence of microscopic flaws in the single sapphire crystals used for the tubes.

Capillary NMR tube cells have been constructed by Yonker and coworkers for use in commercial spectrometers [5]. The capillary cell is constructed of up to 42 windings of fused silica capillary tubing, which fits into a commercial 5 or 10 mm NMR tube. The small internal volume of this capillary cell allows high pressures to be achieved with relative safety.

The use of metallic vessels in NMR spectroscopy began over 40 years ago [6]. The design of a variety of such probes has been previously reviewed [1]. A

---

*Corresponding author. Fax: +1-6302529373; e-mail: rtahke@cmt.anl.gov

0920-5861/99/$ – see front matter © 1999 Elsevier Science B.V. All rights reserved.
PII: S0920-5861(98)00448-9

disadvantage to this approach is the degree of specialized equipment needed. Current designs require the use of wide-bore NMR magnets and the fabrication and assembly of non-standard NMR probes and pressure vessels. The use of compact, high-pressure NMR probes will be presented here whose design is based on toroid detector coils and cavities.

An excellent design for metallic NMR probes employs toroid detectors in place of the traditional Helmholtz detector used in commercial NMR spectrometer probes [7]. Difficulties arise in the design of metallic probes using Helmholtz coils as the diameter of the pressure vessel must be approximately three times that of the coil to minimize magnetic coupling with the walls of the containment vessel [8,9]. The advantages of the toroid detector are its greater intrinsic coil efficiency [10] and its containment of the magnetic field (B1) lines *within* the toroid coil. These allow the design of high-pressure vessels with high signal-to-noise ratios, as there is only a minimal magnetic coupling with the walls of the metal containment vessels. This is in spite of the fact that the detector extends out to near the metallic walls, as shown in Fig. 1. The use of toroid detectors allows for the design of smaller pressure vessels in which the most efficient use of sample is attained. The less cumbersome pressure vessels free up the additional space required for the design of a high-pressure probe with high-temperature capabilities. The toroid detector can be either a wire coil or a machined cavity [7,11]. High-pressure toroid NMR probes can be routinely operated at 300 atm and up to 250°C. Such operating conditions make it extremely well suited for the examination of homogenous catalytic processes that are industrially important, such as the oxo process.

The oxo process uses homogeneous catalysts for the hydroformylation of olefins and is one of the largest industrial processes used worldwide today [12]. In this process, carbon monoxide and hydrogen react with an olefin to selectively produce the desired linear isomers of aldehydes (see Eq. (1)). The linear 'normal' isomers are desired over the branched 'iso' aldehyde products. The capacities of homogeneous oxo processes exceeded 6.6 million tons per year in 1995 with the products used in the manufacture of detergents, plastics, and agricultural products [13].

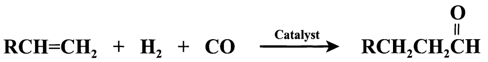

$$\mathrm{RCH{=}CH_2 + H_2 + CO \xrightarrow{Catalyst} RCH_2CH_2\overset{\overset{O}{\|}}{C}H} \qquad (1)$$

While rhodium catalysts account for most of the C_4 hydroformylation products, oxo reactions producing

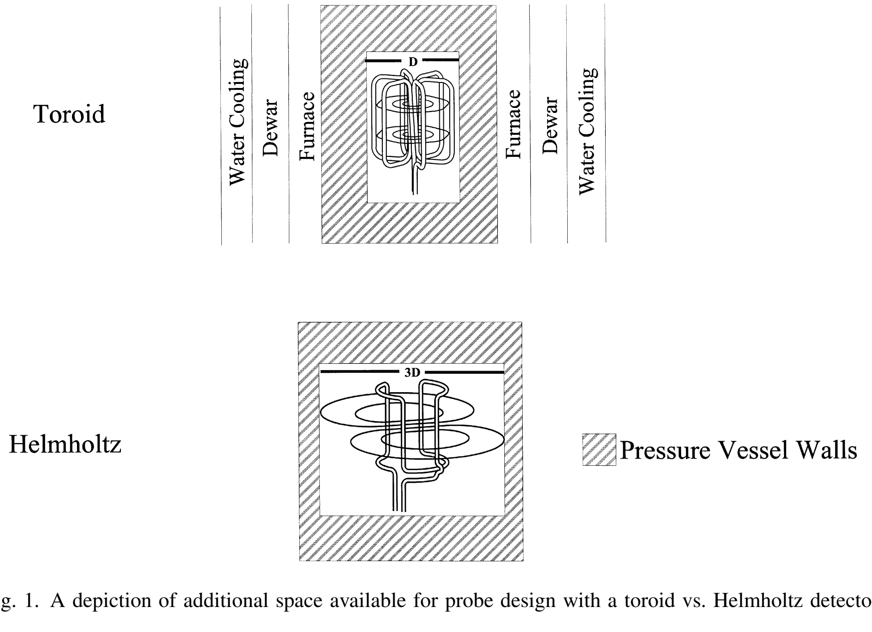

Fig. 1. A depiction of additional space available for probe design with a toroid vs. Helmholtz detector.

C_5 and higher products are dominated by cobalt catalysts by a ratio of 9 to 1. The primary advantage of cobalt catalysts over rhodium is their better reactivity toward internally branched olefins. The thermal stability of the cobalt catalysts is also desirable as high temperatures are required for separation of high molecular weight products by distillation. Phosphine-modified cobalt catalysts greatly improve the ratio of normal-to-iso products and now account for 0.7 million tons of products per year [13].

Our previous studies of the hydroformylation reactions were based on dicobalt octacarbonyl, $Co_2(CO)_8$, in supercritical carbon dioxide ($scCO_2$) [14]. Supercritical carbon dioxide is an ideal medium for use in performing and monitoring catalysis by NMR due to the high diffusivities and low viscosities of supercritical fluids. These properties give supercritical fluids gas-like mass transport properties while retaining liquid-like solvating power. In catalysis, $scCO_2$ solvent systems have also been shown to increase selectivity in hydroformylation and asymmetric hydrogenation reactions [14,15].

The $scCO_2$ solvent has also proven advantageous for the monitoring of cobalt-containing species by ^{59}Co NMR due to its low viscosity [16–18]. Specifically, compelling evidence for the formation of $^{\bullet}Co(CO)_4$ radicals under hydroformylation conditions has been observed. Application of ^{59}Co NMR spectroscopy allowed the observation of a facile hydride ligand exchange that equilibrates the cobalt centers of $Co_2(CO)_8$ and $HCo(CO)_4$. This exchange reaction manifests itself in a line-broadening effect and ultimately the coalescence of the corresponding dimer and hydride resonances. In addition, a contact shift was observed for the chemical-shift average resonance of free carbon monoxide and $Co_2(CO)_8$ in ^{13}C NMR spectra. Further support for the presence of cobalt tetracarbonyl radicals came from magnetic susceptibility measurements, which were correlated with the homolysis of the cobalt–cobalt bond in dicobalt octacarbonyl [17,18].

The presence of a significant amount of cobalt carbonyl radicals under hydroformylation conditions is important as radicals are not considered by the conventional hydroformylation mechanism proposed by Heck and Breslow [19,20]. There are also experimental observations which cannot be accounted for by the traditional mechanism. Results from isotope-labeling studies [21] using deuterium gas in place of hydrogen have proven to be unexplainable by this mechanism. There have also been reports of inverse kinetic isotope effects in hydrogenation by olefinic bonds conjugated to aromatic rings [22], presumably due to a hydrogen atom transfer mechanism. In addition, radicals have been suggested to explain the 0.5 order dependence on $Co_2(CO)_8$ for the hydrogenation and hydroformylation of 1-heptene, cyclohexene, and ethylacrylate [23].

There have been reports of kinetic evidence for radicals in the phosphine-modified cobalt carbonyl systems. Brown et al. have proposed a radical chain mechanism for the substitution of phosphines in $Co_2(CO)_8$ to produce $[Co(R_3P)(CO)_3]_2$ [24]. Given the greater electron-donating abilities of phosphines versus carbonyls, the formation of phosphine-substituted radicals seems likely under hydroformylation conditions. Prior to this work, the in situ observation of phosphine-modified cobalt carbonyl hydroformylation catalysts was limited to infrared (IR) spectroscopy at high pressure and temperature [25–27]. The use of in situ ^{31}P NMR spectroscopy offers a new technique which complements in situ IR techniques by allowing observation of the phosphine ligands instead of the convoluted carbonyl resonances observed by IR.

2. Experimental

Equilibrium reactions were examined in situ using a General Electric GN 300/89 NMR spectrometer equipped with a toroid detector pressure probe built in house. Various detailed designs of such probes have been previously described [7,14]. The pressure vessel portion of the probe was machined from Be–Cu alloy (Brush–Wellman alloy 25) and had an 8 ml volume. The toroid detector (inner radius, 2 mm; outer radius, 6.5 mm; height, 15 mm) was fabricated from three turns of 20 gauge Teflon-coated copper magnet wire (Phoenix Wire) and was double-tuned to ^{1}H (at 300.5 MHz) and an X nucleus (^{13}C, ^{31}P, and ^{59}Co at 75.6, 121.6, and 71.1 MHz, respectively) by means of the hybrid circuit shown in Fig. 2. The f_x part of the circuit (for observation of X nuclei) consists of the toroid coil and variable capacitors (C_1 and C_2) in a standard tapped parallel tuned circuit arrangement. The proton observe channel (f_H) consists of a 3/4

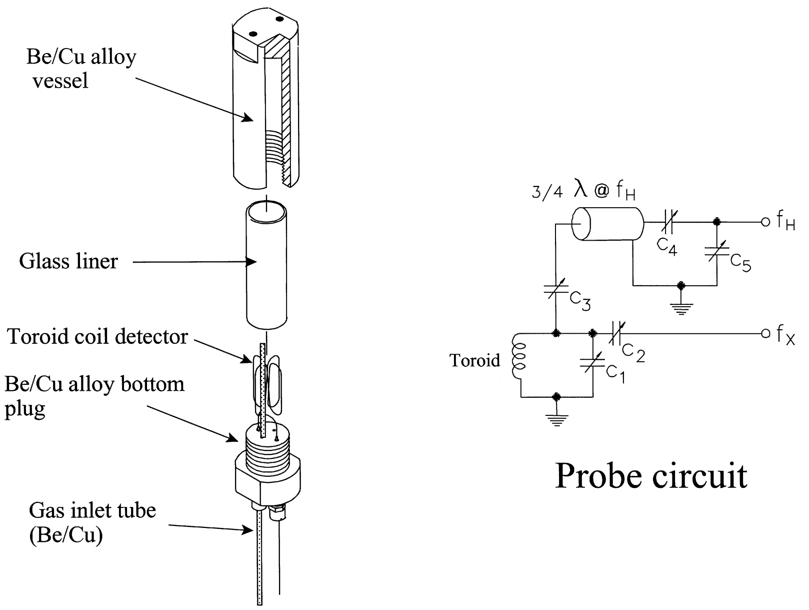

Fig. 2. Toroid pressure NMR probe schematic and probe circuit diagram.

wavelength transmission line in series with C_4 and C_5 in a parallel arrangement. Maximum sensitivity is achieved by incorporating the entire circuit in a capacitor box affixed to the bottom of the pressure vessel in a copper probe housing. All the variable capacitors (C_1–C_5) can be adjusted while being assembled as part of the probe in the magnet by means of extension handles. This allows tuning and matching of the probe to different NMR active nuclei while in use at high pressures and temperatures. The non-magnetic trimmer capacitors used in the tuning circuit were purchased from Voltronics ($C_1 = 0.4$–2.5 pF, #NMQM3 GE, and $C_2 = C_3 = C_4 = 2.0$–120.0 pF, #NMRM120 GE). Probe heating was accomplished by means of an outer-jacketed electrical furnace that fit snugly around the pressure vessel and was powered from a Sorensen DCR150-3B power supply and computer controlled to within ±0.1°C using a copper–constantan thermocouple built into the furnace. The furnace was constructed from a heating element made up of insulated constantan wire non-inductively wound around a copper tube, which fit snugly around the pressure vessel. The furnace was surrounded by a Dewar enclosure and the outside of the entire furnace was cooled by means of a circulated cooling water jacket that prevented disadvantageous heat transfer to the superconducting high-field NMR spectrometer magnet.

A Be–Cu gas tube (1/16 in. diameter) provided a means of pressurizing the sample vessel while the high-pressure probe was assembled within the NMR magnet. The gas tube was connected to a high-pressure manifold outside the superconducting magnet in which accurate pressures were attained and controlled by use of a syringe pump.

Supercritical fluid experiments were performed by initially loading cosolvents and/or cobalt carbonyl complexes into the pressure vessel prior to assembly under a purified helium atmosphere in a glovebox. Reactive and/or inert gases were then admitted to the desired pressures followed by heating to 34°C and introduction of carbon dioxide until a pressure increase of at least 75 atm was attained ($T_{\mathrm{critical}} = 31.3^\circ$C, $P_{\mathrm{critical}} = 72.9$ atm). Pressures were monitored using a strain-gauge pressure transducer (Omega, Model PX302-5KGV) and were controlled by means of an ISCO model 100DM high-pressure syringe pump.

Organic solvents were loaded into the pressure vessel with the cobalt carbonyl complexes under a helium atmosphere in a glovebox. Gases were then admitted under pressure, which was controlled by the high-pressure syringe pump. After the probe was heated and thermally equilibrated, a period of 24 h was given for the gas phase to equilibrate with the liquid solvent.

Dicobalt octacarbonyl and tri-*n*-butylphosphine were purchased from Strem Chemicals and used without further purification. Phosphine-substituted cobalt carbonyl complexes were prepared from dicobalt carbonyl and tri-*n*-butylphosphine with modifications to previously reported methods. Standard Schlenk techniques with respect to handling air-sensitive compounds were followed [28]. All solvents were purchased from Aldrich and were anhydrous, packed under nitrogen in Sure/Seal^{TM} bottles, and used without further purification. Exceptions were benzene-d_6 and cyclohexane, which were used after degassing via freeze/pump/thaw cycles at −78°C. All gases used were purchased from AGA Gas and were at least 99.99% pure. The phosphine-substituted cobalt carbonyl complexes were prepared as follows.

2.1. $[Co(n\text{-}Bu_3P)_2(CO)_3][Co(CO)_4]$ (**4**) [29,30]

Under a carbon monoxide atmosphere, 2 g (5.85 mmol) of dicobalt octacarbonyl was dissolved in 40 ml of toluene. Tri-*n*-butyl phosphine was dissolved in 10 ml toluene under helium and was added to the solution of dicobalt octacarbonyl via cannula transfer. The addition of phosphine was coincident with the liberation of gas (presumably carbon monoxide). The solution was stirred for several hours and was then refrigerated overnight, resulting in the formation of the yellow crystalline product. The identity of the product was confirmed by comparison to the previously reported infrared spectrum [20]. IR (KBr): 1998 cm^{-1} (s), 1982 cm^{-1} (s), 1879 cm^{-1} (vs).

2.2. $[Co(n\text{-}Bu_3P)(CO)_3]_2$ (**1**) [31]

Under an argon atmosphere, 2 g of $[Co(n\text{-}Bu_3P)_2(\text{-}CO)_3][Co(CO)_4]$ (**4**) was suspended in 50 ml of toluene. This suspension was heated until the solid was dissolved, giving a yellow solution. This yellow solution was then gently refluxed for approximately 2 h until it became dark red. The solution was then cooled to room temperature, and the toluene solvent removed by vacuum. The remaining solid was then dissolved in petroleum ether and filtered. This solution was then refrigerated overnight to yield a red crystalline product. The identity of the product was confirmed by comparison to the previously reported infrared spectrum [24]. IR (hydrocarbon solvent): 1970 cm^{-1} (s), 1950 cm^{-1} (vs).

2.3. $Co_2(n\text{-}Bu_3P)(CO)_7$ (**3**) [32]

The monosubstituted dinuclear phosphine complex was prepared from the stoichiometric reaction of dicobalt octacarbonyl with $[Co(n\text{-}Bu_3P)(CO)_3]_2$ (**1**) and confirmed by its IR spectrum as previously reported [32]. The complex was prepared in situ as NMR samples in benzene-d_6. IR (hydrocarbon solvent): 2078 cm^{-1} (s), 2021 cm^{-1} (s), 1992 cm^{-1} (vs), 1954 cm^{-1} (s).

2.4. $HCo(n\text{-}Bu_3P)(CO)_3$ (**2**)

This hydride was prepared in situ in high-pressure NMR experiments by the reaction of $[Co(n\text{-}Bu_3P)(CO)_3]_2$ (**1**) with hydrogen in the presence of carbon monoxide. Alternatively, this hydride was prepared from the reduction of **1** with sodium naphthlanide or sodium amalgam, followed by protonation with triflic acid as an NMR sample under a helium atmosphere similar to prior reports [30]. Its identity was confirmed with the previously reported ^1H NMR spectrum [Co–H, −10.2 ppm ($J_{H\text{–}P} = 47$ Hz) vs. tetramethylsilane] [33].

The ^{31}P NMR chemical shifts were determined (versus external phosphoric acid) as follows for the independently synthesized complexes in benzene-d_6 under 1 atm of helium at room temperature: 53.7 ppm, $[Co(n\text{-}Bu_3P)(CO)_3]_2$ (**1**); 52.4 ppm, $[Co(n\text{-}Bu_3P)_2(\text{-}CO)_3][Co(CO)_4]$ (**4**); 56.0 ppm, $Co_2(n\text{-}Bu_3P)(CO)_7$ (**3**); 43.2 ppm, $HCo(n\text{-}Bu_3P)(CO)_3$ (**2**).

3. Results and discussion

The first phosphine-substituted cobalt carbonyl complexes were prepared by Hieber and coworkers approximately 40 years ago [34,35]. These types of complexes were examined for hydroformylation activity and subsequently patented by Slaugh and Mullineaux at Shell Chemical Company [36,37]. The Heck and Breslow mechanism has been generalized and extrapolated to the phosphine-modified system in which the precatalytic species is the mono-substituted hydride, $HCo(R_3P)(CO)_3$. The hydride is formed from reaction of hydrogen with the dimer, $[Co(R_3P)(CO)_3]_2$. The greater selectivity of the phosphine-modified systems for linear products is attributed to steric effects imparted to the catalyst by the bulky phosphine [12,13].

By far, the most extensively studied phosphine-substituted cobalt carbonyl complexes are those based on tri-*n*-butyl phosphine [38]. It was our hope to extend our high-pressure/high-temperature NMR studies in $scCO_2$ to this phosphine-modified system. While use of the supercritical solvent systems is desired, difficulties with catalyst solubilities have arisen in preliminary experiments and led to the examination of $scCO_2$ with toluene as a cosolvent. Our results showed that solubility of the dimer $[Co(n\text{-}Bu_3P)(CO)_3]_2$ (**1**) is enhanced, and it is thermally stable for at least 8 h in $scCO_2$/toluene mixtures, as shown in Fig. 3. However, upon addition of carbon monoxide and hydrogen, the dimer is lost from solution, as shown by the ^{31}P NMR spectrum in Fig. 4. This observation is consistent with the formation of a species that is insoluble in the $scCO_2$/toluene solvent mixture. An investigation of the phosphine-modified system in more traditional organic solvents was, therefore, undertaken.

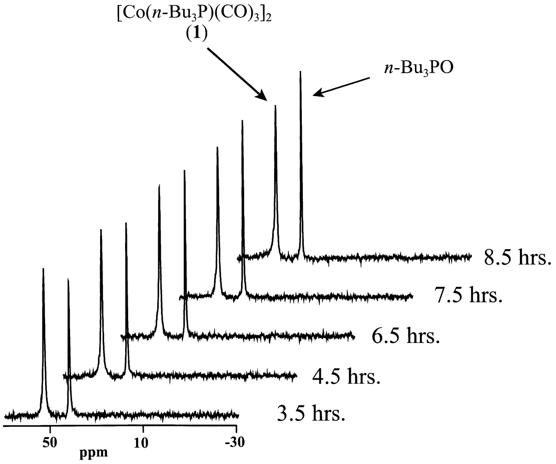

Fig. 3. ^{31}P NMR spectra of $[Co(n\text{-}Bu_3P)(CO)_3]_2$ in CO_2/toluene (10 : 1) at 100°C with tri-*n*-butyl phosphine oxide added as an integration standard.

By moving from supercritical fluids to organic solvents, problems with respect to mass transfer are encountered. The most dramatic of these is the dissolution of gaseous reactants into the organic phase. The degree of this problem in an 8 ml pressure vessel is shown in Fig. 5, in which 6 ml of benzene is pressurized with 100 atm of hydrogen. In a supercritical phase this would correspond to a concentration of approximately 4 M in hydrogen. At equilibrium, the concentration in the benzene liquid phase is only

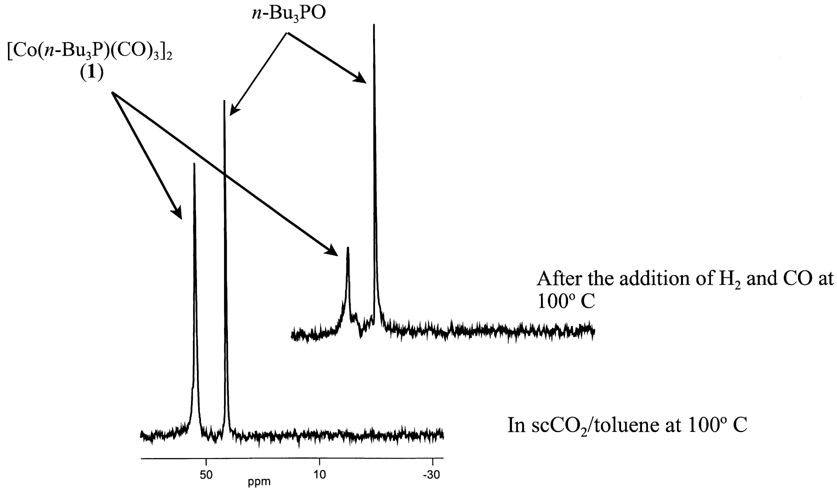

Fig. 4. ^{31}P spectra showing the loss of dimer (**1**) from $scCO_2$/toluene (10 : 1) in the presence of synthesis gas.

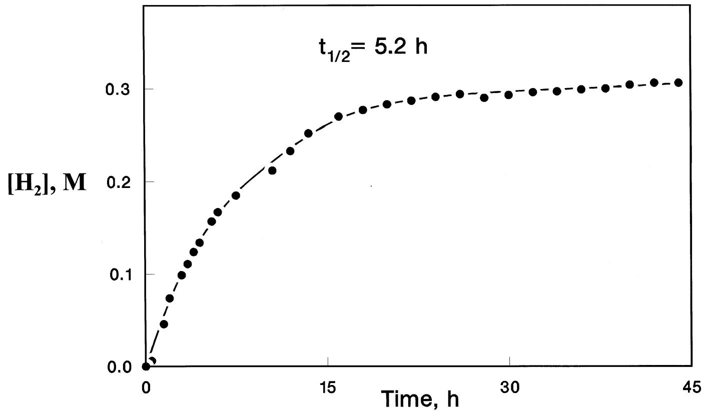

Fig. 5. The time dependence of the dissolution of H_2 into 6 ml C_6D_6 at 100 atm in an 8 ml pressure vessel.

0.3 M. Even more striking is the time required to achieve equilibrium between the benzene and the gaseous hydrogen phase. The hydrogen is dissolved into the benzene with a 5.2 h half-life. In most cases, this corresponds to a period of at least 24 h for equilibrium to be achieved, and this time constraint severely limits the monitoring of rates of reaction. It has been found that this half-life is dependent upon cell configuration, i.e., upon the volumes for solvent and gaseous head space [39].

To overcome gas–liquid phase mixing problems, toroid NMR probes with agitation mechanisms are under development [39]. One type of agitator, making use of the B_0 field of the superconducting NMR magnet, consists of a copper coil form wrapped with 50 windings of a single-strand magnet wire (32 gauge, Teflon, quad-coated copper). The application of an AC current to this agitator coil form causes its movement due to the alignment of its resultant oscillating magnetic field within the static B_0 field of the NMR magnet. A

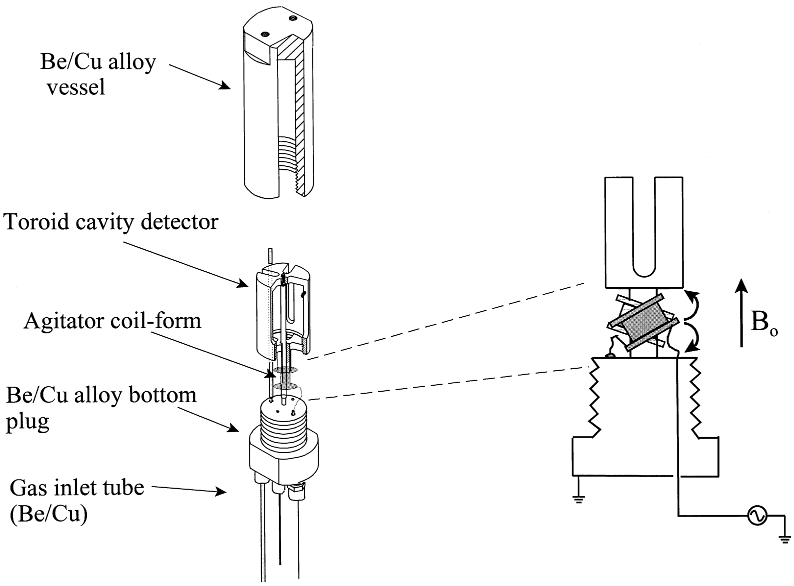

Fig. 6. Schematic of agitator mechanism in a toroid cavity NMR probe.

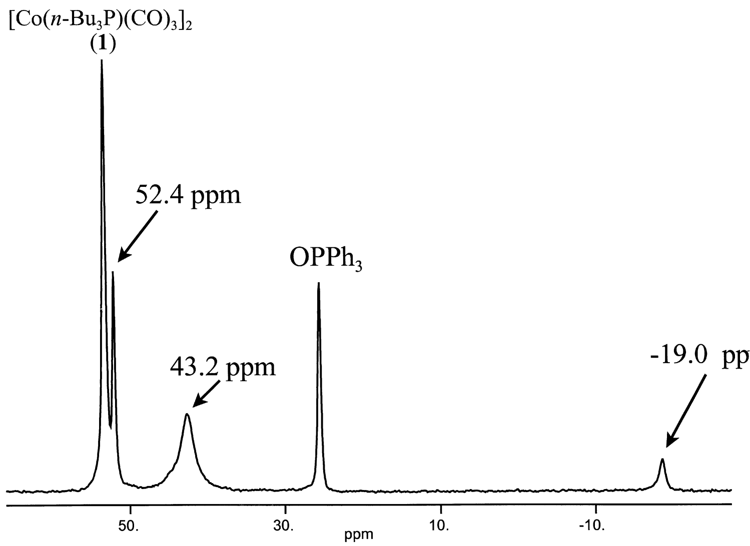

Fig. 7. ${}^{31}P$ spectrum of products from the reaction of $[Co(Bu_3P)(CO)_3]_2$ (**1**) under 138 atm of 1 : 1 H_2/CO in C_6D_6 at 100°C with triphenylphosphine oxide added as an integration standard.

schematic of this agitator is shown in Fig. 6. This agitator has not yet been used for kinetic or equilibrium measurements and is still under development.

There is a notable absence of conventional ${}^{31}P$ NMR spectroscopic data in the literature on $[Co(n\text{-}Bu_3P)(CO)_3]_2$ (**1**) and related complexes. Given the lack of ${}^{31}P$ NMR data available, we undertook the task of examining the dimer and related species from in situ high-pressure reactions and at ambient conditions by independent syntheses of species when possible.

The reactivity of $[Co(n\text{-}Bu_3P)(CO)_3]_2$ (**1**) under a 1 : 1 mixture of hydrogen and carbon monoxide at 138 atm was monitored by ${}^{31}P$ NMR spectroscopy in benzene at 100°C. The ${}^{31}P$ NMR spectrum in Fig. 7 shows three new resonances ($\delta = 43.2$, 52.4, and -19 ppm) upon equilibration of **1** (at $\delta = 53.7$ ppm) with hydrogen and carbon monoxide in benzene-d_6 under these conditions.

The resonance at $\delta = 43.2$ ppm is only observed in the presence of hydrogen, while the remaining two resonances are also present under high pressures of carbon monoxide in the absence of hydrogen. The resonance at $\delta = 43.2$ ppm arises from the mononuclear phosphine-substituted hydride $HCo(n\text{-}Bu_3P)(CO)_3$ (**2**) [30,33,38]. The hydride is also evident in the ${}^{1}H$ NMR occurring at $\delta = -10.2$ ppm ($J_{H\text{–}P} = 47$ Hz), as previously reported [30,33].

The simplest reaction which **1** could undergo with carbon monoxide is that of carbon monoxide substitution for $n\text{-}Bu_3P$, as shown in Eq. (2), to form the monophosphine-substituted dinuclear complex, $Co_2(n\text{-}Bu_3P)(CO)_7$ (**3**). However, the chemical shifts of the new species at $\delta = 52.4$ ppm and $\delta = -19$ ppm (Fig. 7) do not correspond to that of **3** ($\delta = 56.0$ ppm at ambient temperature) and free tri-n-butyl phosphine ($\delta = -31$ ppm). The mono-substituted dicobalt carbonyl complex **3** was prepared independently, as reported in the literature [40], and it exhibits a ${}^{31}P$ NMR chemical shift dependence on temperature [41]. This behavior is inconsistent with any of the species observed upon the reaction of **1** with carbon monoxide and hydrogen. Instead, the new resonance at $\delta = 52.4$ ppm corresponds to that of the disproportionation salt $[Co(Bu_3P)_2(CO)_3]^+$-$[Co(CO)_4]^-$ (**4**) as formed in Eq. (3). This assignment was confirmed by the observed ${}^{31}P$ NMR chemical shift of an authentic sample of **4** in benzene-d_6. The resonance at $\delta = -19$ ppm, while closer to that of free phosphine at -31 ppm, is still far removed from that of free phosphine.

$$\underset{\mathbf{1}}{[Co(n\text{-}Bu_3P)(CO)_3]_2} + CO \rightleftharpoons \underset{\mathbf{3}}{Co_2(n\text{-}Bu_3P)(CO)_7} + n\text{-}Bu_3P \qquad (2)$$

$$\underset{\mathbf{1}}{[Co(n\text{-}Bu_3P)(CO)_3]_2} + CO \rightleftharpoons \underset{\mathbf{4}}{[Co(n\text{-}Bu_3P)_2(CO)_3][Co(CO)_4]} \qquad (3)$$

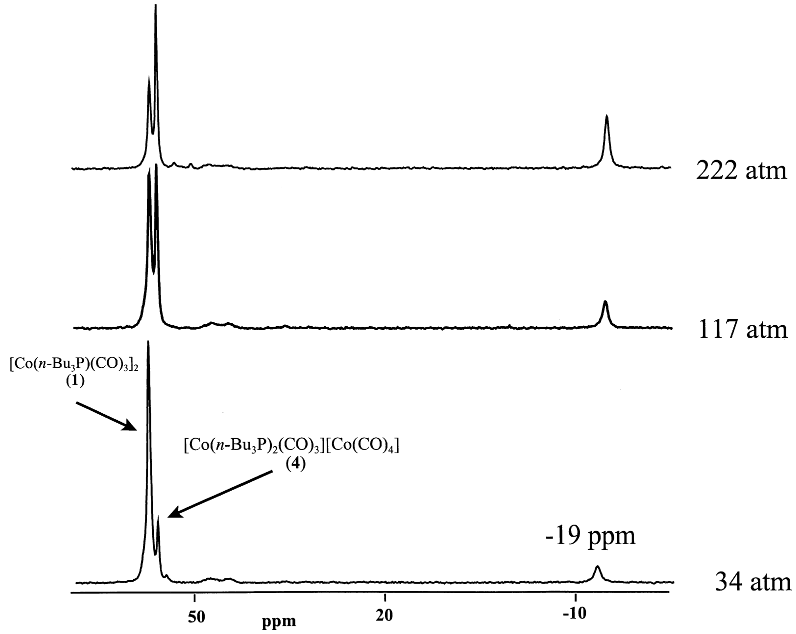

Fig. 8. ^{31}P NMR spectra demonstrating the CO pressure dependence of the equilibria of dimer (**1**), salt (**4**), and −19 ppm species.

The formation of the disproportionation salt **4** and the species corresponding to the $\delta = -19$ ppm resonance is reversible and is favored with increasing carbon monoxide pressures, as shown in Fig. 8. Pronounced solvent and temperature effects on these equilibria are apparent as observed by the ^{31}P NMR spectra in Figs. 9 and 10.

Only two ^{31}P NMR resonances are observed when **1** equilibrates with carbon monoxide in cyclohexane at 100°C (in addition to the internal reference tri-*n*-butylphosphine oxide). These resonances are due to **1** and the unidentified species at $\delta = -19$ ppm. The absence of $[Co(Bu_3P)_2(CO)_3][Co(CO)_4]$ (**4**) in the spectrum obtained in cyclohexane is consistent with **4** being a polar species (i.e., salt). A sample of authentic **4** was not appreciably soluble in cyclohexane (at room temperature). The resonances due to **1**, **4**, and the unidentified species at $\delta = -19$ ppm are all significant in benzene. The increased polarity of dioxane versus benzene leads to a shifting of the equilibrium from **1** to the formation of more **4**. Even at very high pressures of carbon monoxide, there is little of the $\delta = -19$ ppm species present in dioxane at 100°C. The increased polarity of i-butanol greatly favors the formation of **4**, with no dimer **1** present except at very low carbon monoxide pressures and high temperatures. No indication of the unidentified species was observed at any temperature or pressure of carbon monoxide in i-butanol. These observations on solvent polarity demonstrate that the dimer and species giving rise to the resonance at $\delta = -19$ ppm are favored in non-polar solvents, while the salt **4** is greatly favored in polar solvents.

The temperature effects follow the same general trend, as shown in Fig. 10, for all solvents examined. The salt **4** and the unidentified species are favored at lower temperatures, whereas the dimer **1** is favored at higher temperatures. At temperatures below 75°C, a new resonance grows into the ^{31}P NMR spectrum. Fig. 11 shows the ^{31}P NMR spectra under similar conditions at 20°C and 100°C in toluene. At 20°C two separate resonances ($\delta = 52.9$ and $\delta = 52.4$ ppm) can be seen in Fig. 12. If the pressure of carbon monoxide is reduced at these lower temperatures, the resonance at $\delta = 52.9$ ppm slowly decreases. The complex at $\delta = 52.9$ ppm proved to be unisolable due to its instability at low carbon monoxide pressures. The observation that this species only forms

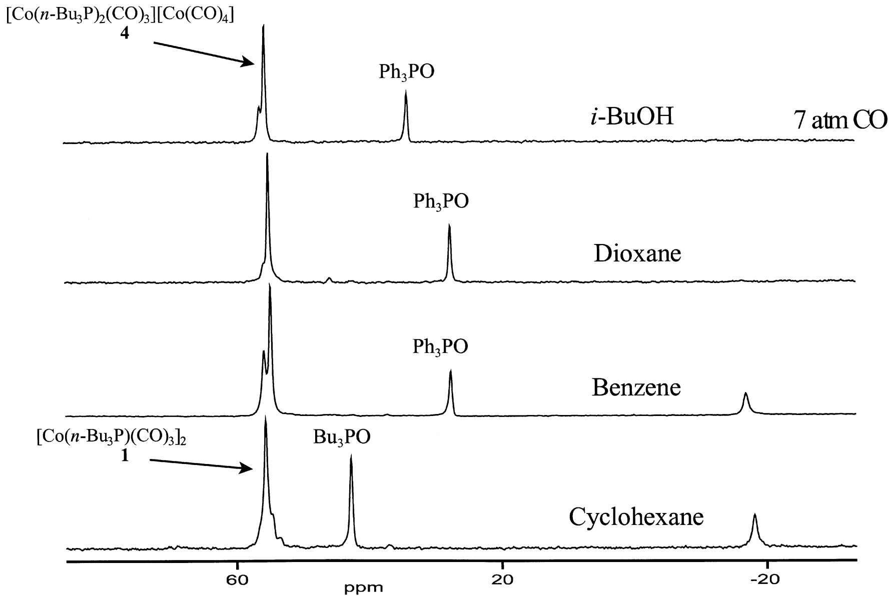

Fig. 9. ^{31}P NMR spectra demonstrating equilibrium species dependence on polarity under 280 atm CO (except in i-butanol, 7 atm CO) at 100°C.

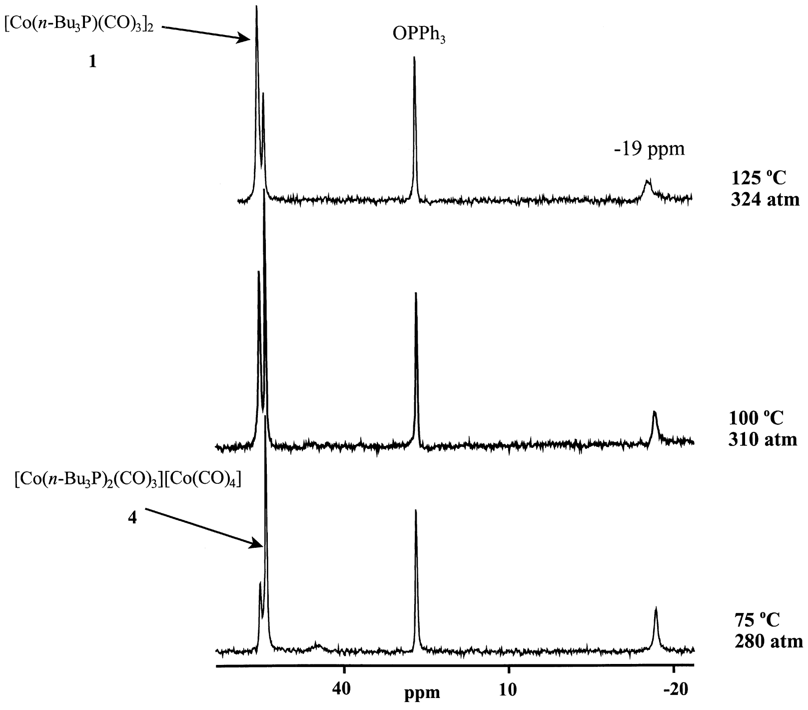

Fig. 10. Temperature dependence of salt (**4**) and −19 ppm species equilibrium in toluene solvent.

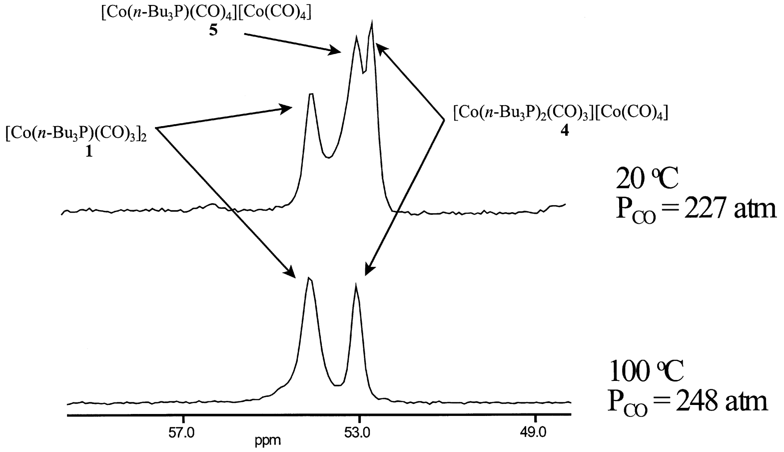

Fig. 11. ^{31}P NMR of dimer/salt species in toluene at 100°C and 20°C at high pressures of CO.

under high pressures of carbon monoxide is consistent with formation of the salt [Co(n-Bu$_3$P)(CO)$_4$]-[Co(CO)$_4$] (**5**). This new species could form from the disproportionation of **3** in Eq. (4), which would explain the lack of observation of **3** under these conditions. This assignment is indirectly supported by the observation that the addition of free n-Bu$_3$P was found to inhibit formation of this new resonance at $\delta = 52.9$ ppm. Free n-Bu$_3$P is often added to dicobalt octacarbonyl in excess of 2 : 1 for added stability of the phosphine-modified cobalt carbonyl system. The free phosphine is presumed to inhibit carbon monoxide substitution at high pressures of carbon monoxide.

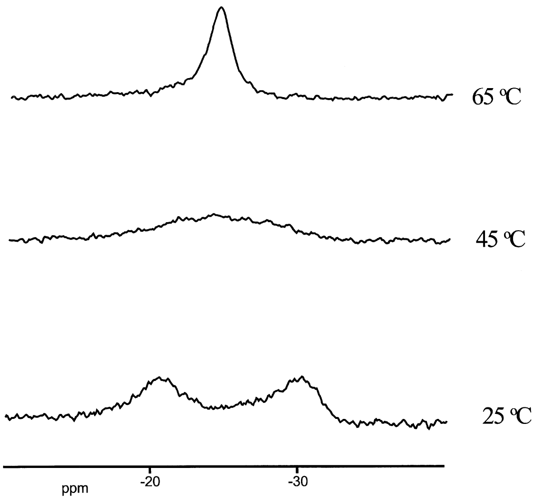

Fig. 12. ^{31}P NMR spectrum showing the resolution of free n-Bu$_3$P from the species at −19 ppm.

$$\underset{\mathbf{3}}{\mathrm{Co_2}(n\text{-}\mathrm{Bu_3P})(\mathrm{CO})_7} + \mathrm{CO} \rightleftharpoons \underset{\mathbf{5}}{[\mathrm{Co}(n\text{-}\mathrm{Bu_3P})(\mathrm{CO})_4][\mathrm{Co}(\mathrm{CO})_4]} \qquad (4)$$

Equilibrium of the salt/dimer in benzene was reexamined in the presence of 1 equivalent of excess free phosphine per dimer **1**. There was little change in the equilibrium, as expected from the lack of phosphine dependence shown in Eq. (3). However, data were obtainable at lower temperatures without complications arising from the new low-temperature resonance at $\delta = 52.9$ ppm.

A change associated with this addition of free phosphine into the high-pressure equilibria is the chemical shift averaging of the unidentified species (originally occurring at $\delta = -19$ ppm) with free phosphine at temperatures above room temperature in the ^{31}P NMR spectra. When the temperature is lowered to 25°C, the free phosphine resonance and the resonance at $\delta = -19$ ppm in the ^{31}P spectra begin to resolve (Fig. 12). There is also a chemical shift dependence of this averaged resonance on carbon monoxide pressure, as shown in Fig. 13. In this series of spectra, the chemical shift of the averaged resonance approaches $\delta = -19$ ppm at high carbon monoxide pressures. This is consistent with increased amounts of the unidentified species forming at higher pressures of

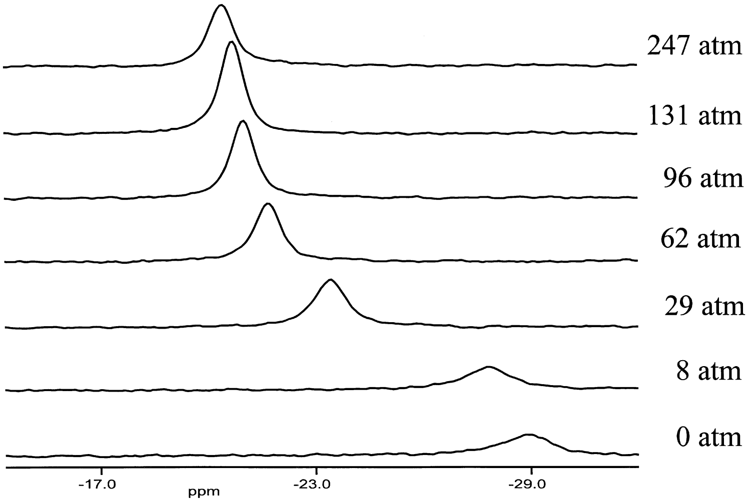

Fig. 13. ^{31}P NMR chemical shift dependence of the chemical-shift-averaged resonance of −19 ppm species and 'free' n-Bu_3P on CO pressure at 100°C.

carbon monoxide. The unidentified species at $\delta = -19$ ppm shows no chemical shift dependence on carbon monoxide pressure in the absence of free phosphine.

Fig. 14 shows the resulting equilibrium species at 125°C under 239 atm of carbon monoxide when the ratio of **1** to free n-Bu_3P is increased to 1 : 4. Almost all of **1** is consumed, and the only other resonance present is that of the shifted free phosphine exchanging with the unidentified species. The conversion of the majority of cobalt-containing species to this species exchanging with free phosphine is a significant observation, as it suggests a change in 'resting state' of the catalyst in the presence of excess phosphine.

Possible identities for this species at $\delta = -19$ ppm are cobalt(II) salts, cobalt-centered radicals, metallo-

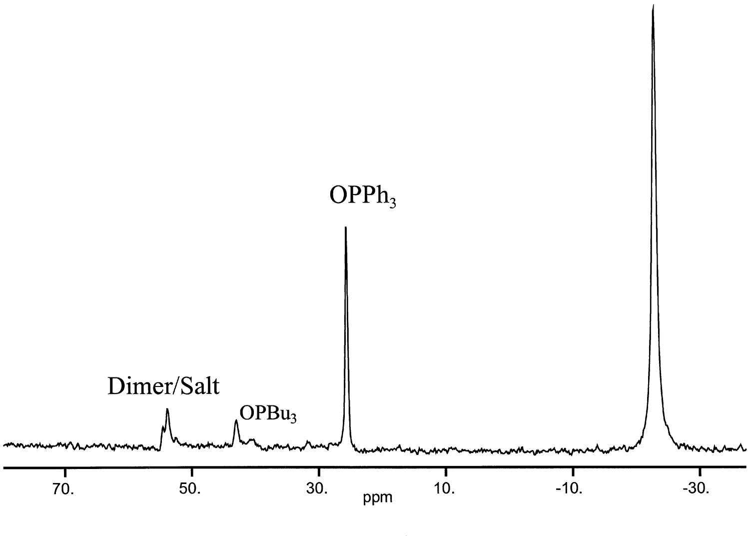

Fig. 14. ^{31}P NMR spectrum of equilibrium species from the reaction of **1** and four equivalents of free n-Bu_3P under 279 atm CO at 125°C.

ketone species, or phosphido cluster complexes. Cobalt(II) salts have been observed to form from dicobalt octacarbonyl with hard Lewis base ligands, such as amines or lower alcohols. No significant electron spin resonance (ESR) signals could be obtained for samples from the high-pressure NMR reactions. This result argues against the formation of a significant amount of Co(II) or cobalt-centered radicals [42]. This is in addition to the fact that the unidentified species is *disfavored* in polar solvents, making it unlikely that this species is a cobalt(II) salt.

The formation of cobalt cluster compounds is unlikely under the conditions of high carbon monoxide pressure. However, such cluster formation has been proposed under hydroformylation conditions for rhodium catalysts containing aryl phosphines [43,44]. Cluster formation in these instances would occur with bridging phosphido ligands resulting from the decomposition of the triarylphosphine ligands. The analogous cobalt clusters are under consideration as possible identities for the species corresponding to the $\delta = -19$ ppm resonance; however, these complexes are inconsistent with the higher thermal stability of the cobalt alkyl phosphine systems, and the formation of these clusters would not be consistent with the reversibility of this complex's formation.

4. Conclusions

High-pressure toroid detector NMR probes have proven to be valuable tools in the examination of the pre-equilibria of phosphine-modified cobalt carbonyl hydroformylation catalysts. The phosphine substitution into these systems increases the complexity of the system far beyond that of simple carbon monoxide substitution for phosphine ligands under high pressures of carbon monoxide. The disproportionation reaction of the dimer $[Co(n\text{-}Bu_3P)(CO)_3]_2$ (**1**) with carbon monoxide to give $[Co(n\text{-}Bu_3P)_2(CO)_3][Co(CO)_4]$ (**4**) is the dominant equilibrium in organic solvents, even in the presence of hydrogen. This reaction becomes irreversible due to the precipitation of the catalyst out of the supercritical carbon dioxide/toluene solvent mixtures. The salt formed from this disproportionation reaction (**4**) is favored at low temperatures and with polar solvents. The issue of solvent polarity is relevant to the catalyzed hydroformylation process, as the aldehyde products are further hydrogenated to give alcohols which increase the polarity of the overall reaction mixture. This increase in polarity may shift the equilibrium to the salt (**4**) from dimer (**1**) and, therefore, away from the hydride (**2**) which enters into the hydroformylation catalytic cycle.

The substitution of carbon monoxide for the phosphine ligands does not appear to be a major equilibrium component of the system, although at temperatures below 75°C there is evidence for the formation of the monophosphine-substituted salt $[Co(n\text{-}Bu_3P)(CO)_4][Co(CO)_4]$ (**5**). The substitution of phosphine ligands by carbon monoxide is undesirable in this system as it forms the cobalt tetracarbonyl hydride, which is less selective for normal hydroformylation products. Formation of this mono-substituted phosphine complex (**5**) can be prevented by the introduction of free phosphine into the system.

In addition to salt formation, an unidentified species is observed in the ^{31}P NMR spectrum at $\delta = -19$ ppm upon reaction of the dimer $[Co(n\text{-}Bu_3P)(CO)_3]_2$ (**1**) with high pressure of carbon monoxide in non-polar solvents. Present in minor amounts in the absence of free phosphine, this species becomes the predominant cobalt-containing species observed in the presence of excess free phosphine. As with formation of the salt (**4**) in polar solvents, formation of this species in the presence of excess free phosphine shifts the equili-

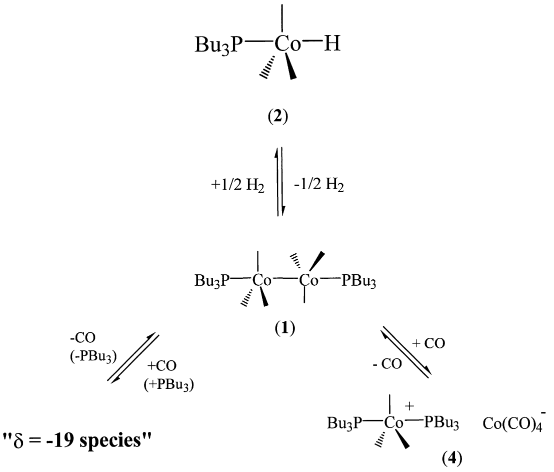

Scheme 1. The predominant equilibria of phosphine-substituted cobalt carbonyls prior to the catalytic hydroformylation cycle (carbonyl ligands are shown as lines for clarity).

brium away from dimer (**1**) and, ultimately, results in a reduced hydride concentration, as depicted in Scheme 1. As these species are in *equilibrium* with the dimer (**1**), they will not prevent formation of the hydride, which is consumed in the irreversible hydroformylation and regenerated. However, by tying up the active cobalt available for hydride formation in these species, the catalytic activity of the system with respect to the amount of cobalt would decrease.

Acknowledgements

The authors thank Professor J. Halpern, Dr. M. Chen, and Dr. T. Krause for helpful discussions. Support for this work was provided by the Office of Basic Energy Sciences, Division of Chemical Sciences, U.S. Department of Energy under contract W-31-109-ENG-38.

References

[1] L. Helm, A.E. Merbach, D.H. Powell, in: W.B. Holzapfel, N.S. Isaacs (Eds.), High-pressure Techniques in Chemistry and Physics: A Practical Approach, Oxford Press, Oxford, 1997, Chap. 4, p. 187.

[2] D.C. Roe, J. Magn. Reson. 63 (1985) 388.

[3] I.T. Horváth, J.M. Millar, Chem. Rev. 91 (1991) 1339.

[4] S. Bai, C.M. Taylor, C.L. Mayne, R.J. Pugmire, D.M. Grant, Rev. Sci. Instrum. 67 (1996) 240.

[5] C.R. Yonker, T.S. Zemanian, S.L. Wallen, J.C. Linehan, J.A. Franz, J. Magnet. Reson. Series A 113 (1995) 102.

[6] G.B. Benedek, E.M. Purcell, J. Chem. Phys. 22 (1954) 2003.

[7] J.W. Rathke, J. Magn. Reson. 85 (1989) 150.

[8] D.I. Hoult, R.E. Richards, J. Magn. Reson. 24 (1976) 71.

[9] D.I. Hoult, P.C. Lauterbur, J. Magn. Reson. 34 (1979) 425.

[10] T.E. Glass, H.C. Dorn, J. Magn. Reson. 52 (1983) 518.

[11] K. Woelk, J.W. Rathke, R.J. Klingler, J. Magn. Reson. A 109 (1994) 137.

[12] J.P. Collman, L.S. Hegedus, J.R. Norton, R.G. Finke, Principles and Applications of Organotransition Metal Chemistry, University Science Books, Mill Valley California, 1987.

[13] M. Beller, B. Cornils, C.D. Frohning, C.W. Kohlpainter, J. Mol. Catal. A 104 (1995) 17.

[14] J.W. Rathke, R.J. Klingler, T.R. Krause, Organometallics 10 (1991) 1350.

[15] M.J. Burk, S. Feng, M.F. Gross, W. Tumas, J. Am. Chem. Soc. 117 (1995) 8277.

[16] A. Carrington, A.D. Mclachland, Introduction to Magnetic Resonance, Harper & Row, New York, 1967, Chap. 11–13.

[17] J.W. Rathke, R.J. Klingler, T.R. Krause, Organometallics 11 (1992) 585.

[18] R.J. Klinger, J.W. Rathke, J. Am. Chem. Soc. 116 (1994) 4772.

[19] R.F. Heck, D.S. Breslow, Chem. Ind. London (1960) 467.

[20] R.F. Heck, D.S. Breslow, J. Am. Chem. Soc. 83 (1961) 4024.

[21] P. Pino, Ann. N.Y. Acad. Sci. 415 (1983) 111.

[22] J.A. Roth, M. Orchin, J. Organomet. Chem. 182 (1979) 299.

[23] G. Pályi, F. Ungváry, V. Galamb, L. Mark, Coord. Chem. Revs. 53 (1984) 37 and references therein.

[24] M. Absi-Halabi, J.D. Atwood, N.P. Forbus, T.L. Brown, J. Am. Chem. Soc. 102 (1980) 6248.

[25] G.F. Pregaglia, A. Andreetta, G. Gregorio, G.F. Ferrari, G. Montrasini, R. Ugo, La Chimica e L'Industria 55 (1973) 203.

[26] R. Whyman, J. Organomet. Chem. 66 (1974) C23.

[27] R. Whyman, J. Organomet. Chem. 94 (1975) 303.

[28] D.F. Shriver, M.A. Drezdzon, The Manipulation of Air-sensitive Compounds, 2nd ed., Wiley, New York, 1986.

[29] N.S. Imyanitov, V.A. Volkov, J. Gen. Chem. USSR (Engl. Transl.) 44 (1974) 2741.

[30] F. Piacenti, A. Andreetta, G. Gregorio, G. Montrasi, G.F. Ferrari, Chimica e Industria 49 (1967) 245.

[31] A.R. Manning, J. Chem. Soc. A (1968) 1135.

[32] P. Szab, L. Fekete, G. Bor, Z. Nagy-Magos, L. Mark, J. Organomet. Chem. 12 (1968) 245.

[33] J.P. Jesson, in: E.L. Muetterties (Ed.), Transition Metal Hydrides, Marcel Dekker, New York, 1971, Chap. 4, p. 75.

[34] W. Hieber, W. Freyer, Chem. Ber. 91 (1958) 1230.

[35] W. Hieber, W. Freyer, Chem. Ber. 93 (1960) 462.

[36] L.H. Slaugh, R.D. Mullineaux, U.S. Patent 3,448,157, 1969.

[37] L.H. Slaugh, R.D. Mullineaux, U.S. Patent 3,448,158, 1969.

[38] R.D.W. Kemmitt, D.R. Russell, in: G. Wilkinson, F.G.A. Stone, E.W. Abel (Eds.), Comprehensive Organometallic Chemistry: The Synthesis, Reactions and Structures of Organometallic Compounds, vol. 5, Pergamon Press, Oxford, 1982, Chap. 34, p. 1 and references therein.

[39] D.E. Fremgen, R.J. Klingler, J.W. Rathke, unpublished results.

[40] P. Szab, L. Fekete, G. Bor, Z. Nagy-Magos, L. Mark, J. Organomet. Chem. 12 (1968) 245.

[41] K.W. Kramarz, R.J. Klingler, J.W. Rathke, unpublished results.

[42] It has been suggested by a referee that because Co–Co bonds are not very strong it may be possible to form a carbonyl-bridged dinuclear complex that has lost its Co–Co bond. The resultant 17-electron cobalt centers would require strong antiferromagnetic spin coupling through the bridging carbonyl ligands to be consistent with the ^{31}P NMR and ESR spectral observations. In addition, a simple dinuclear complex with 17-electron cobalt centers is not sufficient to explain the observed CO dependence for the formation of the species at -19 ppm in the ^{31}P spectra. However, the latter contention would be removed if at least one of the cobalt centers has picked up an additional carbonyl ligand to yield a 19-electron cobalt center..

[43] A.G. Abatjoglou, E. Billig, D.R. Bryant, Organometallics 3 (1984) 923.

[44] A.G. Abatjoglou, E. Billig, D.R. Bryant, Organometallics 3 (1984) 932.